*Journal of the European Ceramic Society* **16** (1996) 1319–1327

PII: S0955-2219(96)00063-5
0955-2219/96/$15.00

# Colloidal Processing of a Mullite Matrix Material Suitable for Infiltrating Woven Fibre Preforms Using Electrophoretic Deposition

A. R. Boccaccini,[a] P. A. Trusty,[b] D. M. R. Taplin[c] & C. B. Ponton[d]

[a]School of Metallurgy and Materials, The University of Birmingham, Birmingham B15 2TT, UK
and Department of Environmental Sciences, University of Plymouth, Plymouth PL4 8AA, UK
[b]IRC in Materials for High Performance Applications, The University of Birmingham, Birmingham B15 2TT, UK
[c]Research Office, University of North London, London N7 8DB, UK
[d]School of Metallurgy and Materials and IRC in Materials for High Performance Applications, The University of Birmingham, Birmingham B15 2TT, UK

(Received 13 December 1995; revised version received 29 February 1996; accepted 14 March 1996)

***Abstract***

*Commercially available alumina and silica precursors for the preparation of mullite ceramic via colloidal processing and viscous transient sintering have been identified, including fumed nanosize powders and colloidal suspensions. These materials were chosen due to the fact that they can be used in the form of a sol, as mullite matrix precursors, to infiltrate woven fibre preforms using electrophoretic deposition. The sintered density of the mullite matrices sintered for 2 h, at the upper temperature for fabricating SiC-fibre reinforced composites (1300°C) is only ≈90% of theoretical. However, by exploiting a viscous flow densification mechanism, it is envisaged that hot-pressing can be used to produce fully dense mullite matrix composites at the required temperatures. Additionally, using a simple pressureless sintering route, almost fully dense (98% of theoretical density) monolithic mullite has been obtained from the pre-mullite powders. A very homogeneous and fine microstructure was achieved by sintering for 5 h at a temperature of ≈1450°C.*


## 1 Introduction

Mullite ($3A1_2O_3.2SiO_2$) has a number of desirable properties for high-temperature structural applications, such as excellent high-temperature strength and creep resistance, very good chemical and thermal stability, a low thermal expansion coefficient and high thermal shock resistance.[1] Thus, mullite is an ideal material for use as matrix in the development of ceramic matrix composites (CMCs) for engineering and structural applications at elevated temperatures. Although considerable progress has been made over the last 10 years in the synthesis and processing of monolithic mullite,[2–4] particulate-, whisker- and platelet-reinforced mullite[1,5–8] and even *in-situ* reinforced mullite matrix composites,[9] there has been much less research work on the fabrication of continuous-fibre reinforced mullite matrix composite.[10–13]

A novel approach for manufacturing SiC woven-fibre reinforced mullite has been developed recently.[14,15] It is based on the colloidal processing of mixed $A1_2O_3$ and $SiO_2$ sols and the infiltration of the fibre mats using a patented electrophoretic deposition (EPD) process.[16] The particular grade of SiC fibre used (Nicalon C607) possesses a carbon coating which enables the fibres to conduct electricity, and, hence, be used as an electrode in an EPD cell. There are a number of requirements, however, that the alumina and silica starting materials must fulfil in order to be useful for composite manufacture using this approach.[14] These are:

(1) Particle size in the nanometre range — for full infiltration of tightly woven fibre mats, the size of the alumina and silica particles must be in the nanometre range (<100 nm).
(2) Stability of the mixed sol — in order for both species to infiltrate the fibre mat, 'composite' heterocoagulated particles must be formed in the sol, i.e. maximum mutual attraction of silica and alumina particles must be achieved. The sol, however, must remain stable, i.e. dispersed, to allow particle mobility in the EPD cell.
(3) Mullite formation and densification at relatively low temperatures — the starting

materials should enable full densification of the mullite composition matrix at relatively low temperatures ($T$ <1300°C), and eventually, enable the use of hot-pressing to complete the densification process.

While starting materials (for mullite production) that fulfil requirements (1) and (2)[14, 15] have been identified, further work is needed to assess whether or not these mullite precursors are capable of forming dense mullite at low temperatures.

The third condition mentioned above suggests the employment of the mullite preparation technique known as transient viscous sintering (TVS).[17] In this approach, the mullite composition matrix material remains amorphous (or weakly crystalline) up to temperatures of 1200°C to allow densification by viscous flow, and then subsequently crystallizes rapidly to yield mullite at temperatures below ≈1300°C. Densification by viscous flow has the additional advantage of allowing the use of hot-pressing, with little or no damage being caused to the fibres during pressing.

TVS has been used in the past by several authors[17–21] using different starting materials. Sacks *et al.*,[17] for example, obtained composite particles which consisted of an inner core of $\alpha$-alumina and an outer coating of amorphous silica. Powder compacts prepared with these particles were sintered at relatively low temperatures (≈1300°C). The $\alpha$-alumina particles used, however, had an average diameter of ≈0·2 $\mu$m, and would therefore be too large to infiltrate woven fibres using EPD.[14] The same can be said of the system studied by Shyu and Chen,[18] who used alumina particles of ≈0·1 $\mu$m. In further studies, Wang *et al.*[19,20] and Miao *et al.*[21] have used sol–gel processing for obtaining mullite ceramics via the TVS mechanism. They were successful in preparing 'composite' particles (i.e. silica-coated alumina particles) on the nanometre scale using controlled heterocoagulation of mixed sols. Owing to the low reactivity of the starting alumina and silica materials employed, however, very high temperatures (≈1550 to 1700°C) were required to complete the mullitization process. In addition, cristobalite formed at lower temperatures, which retarded the densification process. In a further paper, the same authors[22] studied the effect of green density on the densification and mullitization of powder compacts made from the 'composite' particles mentioned. They found that both the crystallization temperature of the amorphous silica layer coated on the surface of alumina powder particles and the subsequent mullitization temperature during TVS decreased with increasing green density. For relatively high green densities (70% of the theoretical), mullitization was completed at 1600°C giving 95–96% of theoretical density in the sintered compacts.[22] Thus, according to the previous results, both the nature of the alumina/silica precursors employed and the processing conditions, including the compact green density, influence the observed TVS behaviour.

In this paper we report on the TVS preparation of mullite ceramics from starting materials which are also suitable for the EPD impregnation of fibre mats and, thus, are potentially useful as matrices in CMCs. However, no deliberate effort was made to prepare the 'ideal' composite particles described above, i.e. silica-coated alumina particles. It was envisaged that the nature and particle size of the precursors selected would allow their mixing as alumina/silica clusters on a scale of approximately 5 to 50 nm which, according to the literature,[23–25] leads to substantial densification and mullitization in the temperature range between 1200 and 1300°C, as desired. This material should be able to serve as a matrix for the SiC-fibre reinforced composites under investigation,[14,26] in which the densification and mullitization stages must be completed at temperatures between ≈1250 and ≈1300°C due to the limited temperature window available for processing without damaging the fibre as explained earlier. Furthermore, the simple pressureless densification route which has been developed in the present work for the preparation of monolithic mullite may be used for fibre-reinforced composites, with the understanding, however, that hot-pressing may be necessary for full densification.

## 2 Experimental Procedure

### 2.1 Starting materials

Different commercially available silica and alumina precursors, in the form of sols or fumed nanosize powders, were used in the preliminary studies to find the optimal starting materials for the complete impregnation of fibre mats using EPD.[27] NaOH–stabilized silica sols were not selected since they are prone to crystallization and cristobalite formation at relatively low temperatures, which prevents full densification of the mullite matrix.[20] In addition, the easy availability, low cost and environmental safety of the materials have also been taken into consideration during their selection. On this basis, organometallic compounds were not considered. Thus, only commercial boehmite and ammonia-stabilized silica sols, and high-purity, fumed alumina and silica nanosize powders remain as suitable precursors. These include:

(1) Fumed amorphous silica (Aerosil OX50, Degussa Ltd, UK) — a spherical particle shape highly dispersed powder with a broad particle size distribution (10 to 100 nm) and average particle size of 40 nm. The pH range in water for achieving a stable sol using this silica was 3·8 to 4·8.
(2) Fumed amorphous silica (Aerosil 200, Degussa Ltd, UK) — a spherical particle shape, highly dispersed powder with a narrow particle size distribution and average particle size of 12 nm. The pH range in water for obtaining a stable sol of this silica was 3·6 to 4·3.
(3) Ammonia-stabilized silica sol (Nyacol 2040 NH4, Akzo-PQ, The Netherlands), containing 40 wt% solid. The pH of the as-received sol was 9 and the average particle size 20 nm.
(4) Boehmite ($\gamma$-AlOOH) sol (Remal A20, Remet Corp., USA), containing 20 wt% solid. The boehmite particles had a mean particle size of 50 nm and a fibrillar morphology. The pH of the as-received sol was 4.
(5) Fumed $\delta$-alumina (Aluminium Oxide C, Degussa Ltd, UK) — a highly dispersed quasi-spherical particle shape alumina powder with average particle size of 13 nm. The pH in water ranged from 4·5 to 5·5.

The mixed silica/alumina sols tested are listed in Table 1, together with the pH at which they are stable.

### 2.2 Processing and characterization

The precursors were mixed in a proportion such that the resulting ceramic after firing would be stoichiometric mullite i.e. 72 wt% alumina – 28 wt% silica. For the preparation of sols I and II the fumed silica nanosize powders were added slowly to the boehmite sol which was stirred continually to avoid powder agglomerates forming in the mixture. Sol I was prepared successfully in this way, with a stable sol being obtained at pH ≈ 4·4. Thus, the pH of the original boehmite sol was changed only a little on the addition of the single-component fumed silica. However, when the two-component fumed silica was added to the boehmite to prepare sol II, the resultant mixture gelled immediately. This is due to the strong electrostatic attraction between the silica and alumina (boehmite) particles occurring at this pH, as discussed later. To prepare sol III, the fumed $\delta$-alumina particles were added slowly to the silica sol whilst stirring continuously. The pH was adjusted to a value of ≈9 by adding dilute $NH_3$(aq) dropwise. Sol IV was prepared by adding the alumina and silica fumed nanosize particles to an aqueous solution of pH ≈ 4·8, which was stirred magnetically for 5 h; note that the $\delta$-alumina particles were added first. Transmission electron microscopy (TEM) was employed using a JEOL 4000 FX-TEM to investigate the spatial distribution and clustering arrangements of the alumina (boehmite) and silica particles in the colloidal suspensions.

After magnetic stirring for 5 h, sols I, III and IV and the gel from sol II were all dried slowly at ≈80°C in a muffle furnace overnight. The dried gels were ground subsequently using an $Al_2O_3$ mortar and pestle and then sieved to obtain a powder with a nominal particle size <63 $\mu$m. The resulting powders were then used for the sintering and crystallization experiments. Green compacts (12 mm diameter; ≈7 mm high) were pressed uniaxially using two different compaction pressures (i.e. 170 and 450 MPa). The geometrical density of the green compacts was determined. These compacts were sintered for 2 h at temperatures between 900 and 1450°C in order to assess both the densification behaviour and the crystalline phase development (heating rate: 20°C $min^{-1}$). Powdered sintered samples were investigated by X-ray diffraction (XRD) analysis using Cu $K_\alpha$ radiation. Microstructural characterization was performed solely on samples of sol I. These samples were prepared by compacting the powder at 450 MPa and firing the resultant compacts at 1200°C for 2 h, followed by 5 h at 1450°C. Selected samples were prepared for reflected light optical microscopy and for scanning electron microscopy (SEM) using a JEOL 6300 SEM and a Hitachi S4000 FEG SEM. Polished samples were etched thermally to reveal the grain structure. SEM was also used to examine the fracture surfaces of fired samples. Differential

**Table 1.** Silica/alumina mixed colloidal suspensions investigated

| *Sol* | *Alumina precursor* | *Silica precursor* | *Comments* |
|---|---|---|---|
| I | Remal A20 | Aerosil OX 50 | stable sol at pH ≈4·4 |
| II | Remal A20 | Aerosil OX 50 and Aerosil 200 in 1:1 proportion by mass | no stable sol was obtained (gelation occurred) |
| III | Aluminium oxide C | Nyacol 2040 NH4 | stable sol at pH ≈9 |
| IV | Aluminium oxide C | Aerosil OX50 and Aerosil 200 in 1:1 proportion by mass | stable sol at pH ≈4·8 |

thermal analysis (DTA) was performed on a 10 mg powdered sample of sol I, at a heating rate of 20°C $min^{-1}$ using a Labtherm Scientific STA-780 DTA/TGA apparatus.

## 3 Results

Table 2 presents a summary of the X-ray diffraction analysis results for the fired samples that were compacted at a pressure of 450 MPa. Only a qualitative study of the crystallization development was conducted and so the crystalline phases are listed only in order of decreasing predominance at each temperature. The samples compacted at 170 MPa showed the same evolution of crystalline phases.

The crystallization behaviour of the samples made from sols I and II is very similar. Up to 1200°C, no mullite formation was detected. The samples from sol II did, however, show the presence of δ-alumina at 1200°C. The presence of δ-alumina in sol I at this temperature should not be ruled out. However, its content must be under the detectability limit of XRD. For sols I and II, mullite was the sole crystalline phase detected at 1300°C and above. In contrast, sol III showed the presence of cristobalite in addition to mullite at 1300°C with mullite already being formed at 1200°C in sol IV, δ-alumina and cristobalite are present at 1200°C and δ-alumina is still present at 1300°C, in addition to mullite. The XRD diffraction patterns of powder compacts made from sol I and sintered at 1200 and 1250°C for 2 h are shown in Fig. 1, indicating that between these two temperatures the mullitization reaction has taken place. The seeming presence of a halo at $2\theta = 20°$ in Fig. 1(b) could possibly indicate the presence of a trace amount of amorphous silica at 1250°C. This halo disappeared at 1300°C, however.

Figures 2(a) and 2(b) present the variation in the sintered density of the compacts as a function of the sintering temperature for the two powder compaction pressures of 170 and 450 MPa, respectively. As expected, the density increases

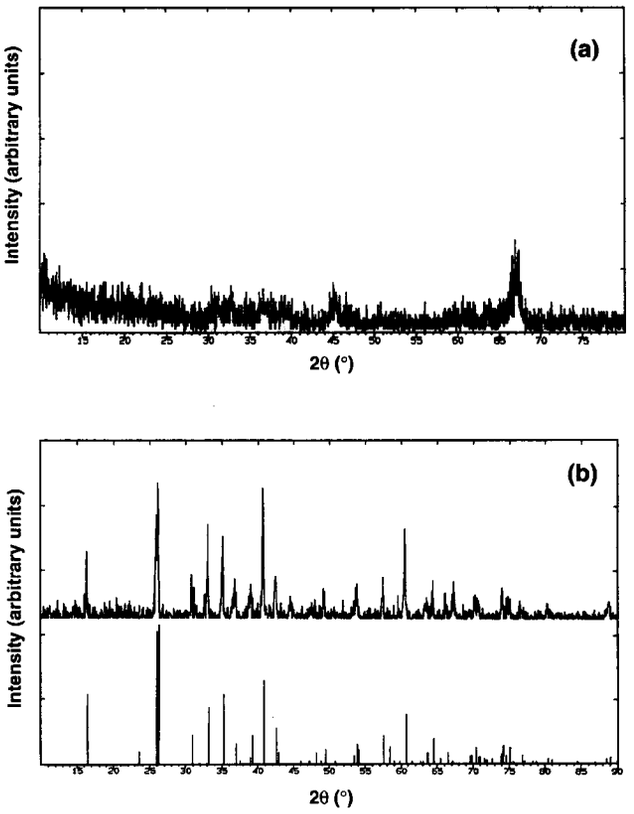


**Fig. 1.** XRD patterns for powder compacts made from sol I and sintered for 2 h at (a) 1200°C and (b) 1250°C, showing that mullitization has taken place within this temperature interval. (The diffraction pattern corresponding to pure mullite is also shown for comparison).

with increasing temperature. It can be seen also that using a higher powder compaction pressure has a positive effect on increasing the final sintered density, as may be expected so long as the compaction pressure is not excessive. A very high compaction pressure may lead to a decrease in the crystallization temperature of the amorphous silica, jeopardising its viscous flow behaviour, and hence, the densification of the compacts at the transient sintering temperature.[20,22]

Since sol I showed the best behaviour, in terms of both densification and crystalline phase development (according to the criteria stated in the Introduction), further in-depth study was restricted to this system.

**Table 2.** Crystalline phases present in the fired samples (as detected by XRD)

| *Sol* | *Temperature (°C)* | | | | |
|---|---|---|---|---|---|
| | *900* | *1100* | *1200* | *1300* | *1450* |
| I | — | — | — | mullite | mullite |
| II | — | — | δ-alumina | mullite | mullite |
| III | δ-alumina | δ-alumina | mullite<br>δ-alumina<br>cristobalite | mullite<br>cristobalite | mullite |
| IV | δ-alumina | δ-alumina | δ-alumina<br>cristobalite | mullite<br>δ-alumina | mullite |

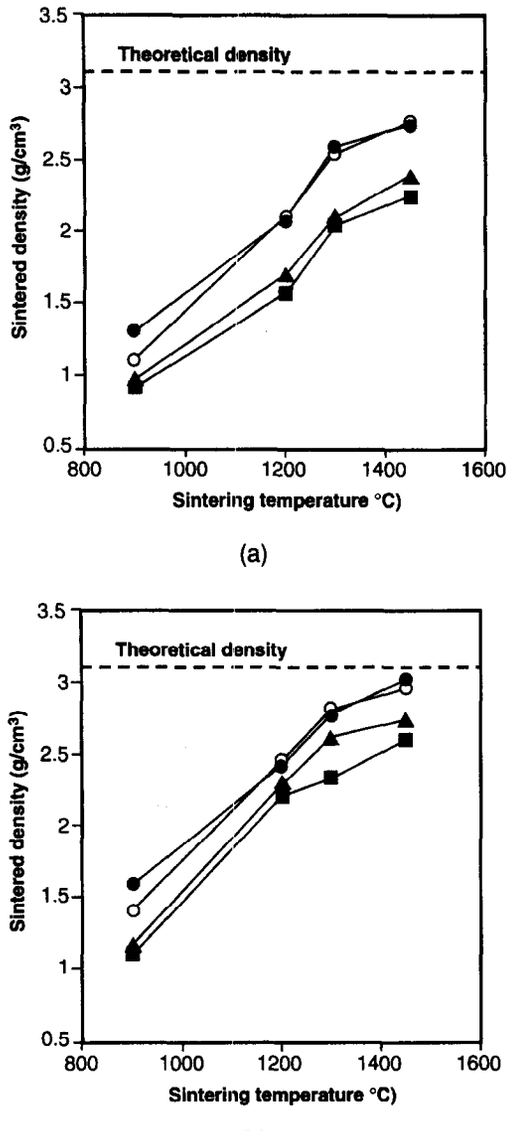


**Fig. 2.** Density of mullite compacts as a function of sintering temperature for two different uniaxial powder compaction pressures: (a) 170 MPa and (b) 450 MPa. Sols I, (●) II, (○) III (▲) and IV. (■).

A TEM photomicrograph of sol I is presented in Fig. 3. It shows clearly the spherical shape of the silica particles and the fibrillar nature of the boehmite sol used. The result of the DTA experiment for sol I is shown in Fig. 4. The broad exotherm between ≈200 and 500°C including the peak at ≈300°C is attributed to the removal of hydroxyl (OH) groups. The curve also exhibited an exothermic peak at ≈1360°C, which is attributed to the formation of mullite. Figure 5 shows the polished surface of a sample fired at 1200°C for 2 h, followed by 5 h at 1450°C. A polished and then thermally etched surface of the same sample is shown in Fig. 6. These micrographs show that the material is almost fully dense, with only some small isolated pores being observed occasionally. In addition, the matrix is composed of very fine equiaxed grains (grain size <≈ 1 $\mu$m). An SEM micrograph of the fracture surface of a

**Fig. 3.** TEM micrograph of sol I at pH ≈4·4 showing the intimate mixture on a nanometre scale of spherical silica and fibrillar boehmite particles.

sample fired at 1200°C for 2 h, followed by 5 h at 1450°C, is shown in Fig. 7; it reveals the homogeneity of the crystalline structure.

## 4 Discussion

On the basis of the XRD results in Table 1, sol I shows the behaviour desired for the preparation of mullite via transient viscous sintering. The material remains amorphous up to temperatures of 1200°C, allowing densification by viscous flow

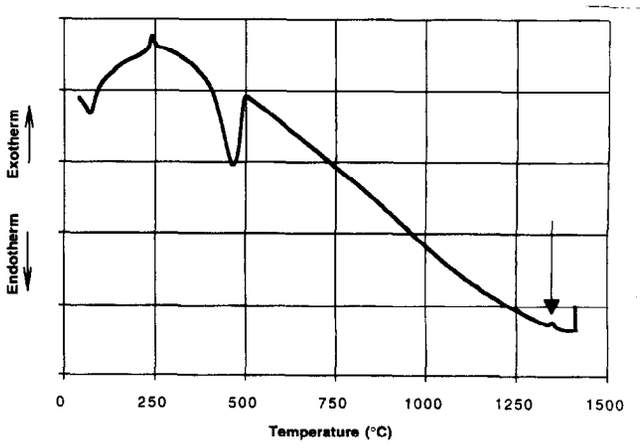


**Fig. 4.** DTA curve for the pre-mullite powder derived from sol I for a 20°C min$^{-1}$ heating rate. The arrow indicates mullite formation at ≈1360°C (exothermic peak).

to take place. The mullitization process is complete at 1300°C, with no other crystalline phases being detectable using XRD. The DTA results for this material are in agreement with the XRD data. The DTA curve showed an exothermic peak at

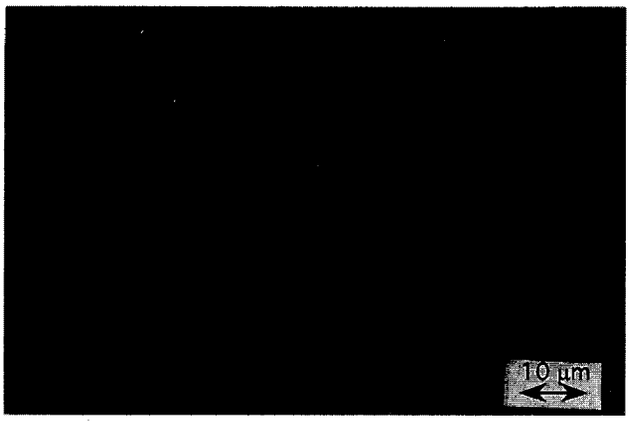


**Fig. 5.** Optical micrograph of a polished section of a mullite sample sintered at 1200°C for 2 h, followed by 5 h at 1450°C, showing that almost full densification was achieved.


**Fig. 6.** SEM micrograph of a polished and thermally etched section of a mullite sample sintered at 1200°C for 2 h, followed by 5 h at 1450°C, showing the very fine and homogeneous microstructure.

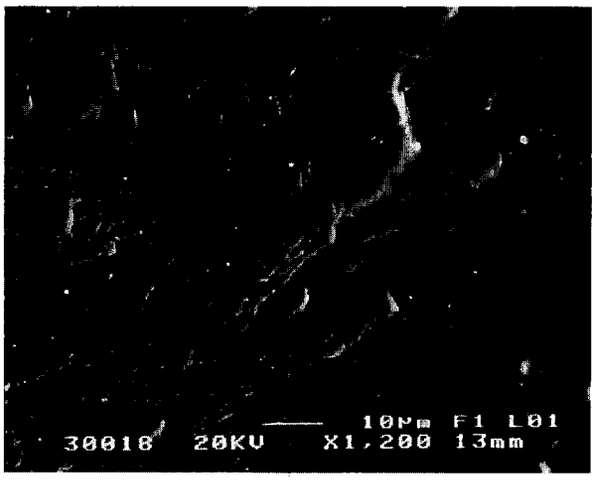


**Fig. 7.** SEM micrograph of the fracture surface of a mullite sample sintered at 1200°C for 2 h, followed by 5 h at 1450°C, showing the homogeneous microstructure.

≈1360°C, which is attributed to the solid-state reaction for mullite formation. The XRD data, however, showed that mullite had formed after 2 h at 1250°C. The discrepancy in these mullite formation temperatures is explained by the isothermal versus the non-isothermal (i.e. constant heating rate) conditions of the sintering and DTA experiments, respectively.

These results are in broad agreement with previous studies on the colloidal processing of mullite.[21–25] Mullite formation in alumina/silica mixtures occurs within different temperature regimes, depending on both the nature of the alumina and silica precursors and the scale of mixing achieved. As stated in the literature, when using colloidal processing, the alumina and silica precursors are present as discrete entities and any chemical reactions between them are of minimal magnitude during gelation. Only at temperatures in excess of ≈1250°C is mullite produced from a mixture of transition (pre-$\alpha$) aluminas, such as $\delta$- or $\theta$-alumina (which are weakly crystalline), and amorphous silica.[23,24] At the pH at which sols I and II were prepared (i.e. pH ≈ 4·4), there is a strong electrostatic attraction between the negatively charged silica and the positively charged boehmite particles, as shown with reference to their zeta potential versus pH curves.[23] Thus, electrostatic attraction is expected to lead to heterocoagulation and the maximum pairing of unlike particles. This behaviour would normally be expected for both sol I and II. The reason why sol II gelled at the same pH is due to the greater number of much smaller silica particles present, since it was a 1:1 mixture of 40 nm and 12 nm average size particles, whereas sol I comprised only 40 nm average size particles. Small particles coagulate more rapidly than large particles because their double layer potential, which is responsible for interparticle repulsion, is much lower than for larger particles suspended in the same medium and, hence, flocculation and gelation can occur more readily.[28] The TEM micrograph of sol I (Fig. 3) confirms that the silica and boehmite particles are mixed intimately on a nanometre scale. It is important to note also that the DTA results for sol I do not indicate the formation of an Al–Si spinel phase at ≈960°C, which has been observed by other authors to be the transitional phase that forms prior to mullite.[4,29–31] Although a TEM characterization of all sols was not conducted, it is reasonable to assume that, due to the nature (primary particle size) of the precursors employed, the scale of alumina/silica mixing is similar for all sols investigated, being in the nanometre range. The shape of the silica- and alumina-bearing precursor particle is, however, different: spherical for the silica

precursors, fibrillar for the boehmite sol (employed in sols I and II) and spherical for the fumed δ-alumina (employed in sols III and IV). This difference in particle morphology could have led to different particle packings during gelation of the sols and consequently to the different crystallization and densification behaviour of sols I and II in comparison with sols III and IV. Moreover, the chemistry of the starting materials in terms of the impurity content and surface reactivity could probably account for such different behaviour also. While sol I and sol II, which show similar crystallization behaviour, were made by starting materials with identical chemical composition, the behaviour of sols III and IV, made from other precursor combinations, was different. Sol III, for example, showed cristobalite formation at a temperature of 1200°C. which may be a consequence of using an ammonia-stabilized silica sol. This cristobalite formation has been reported very frequently in the literature when similar silica sols were used.[21–23,32] In sols I and II cristobalite formation, which has been shown in the literature to retard viscous densification,[20,22] was suppressed by using high-purity fumed silicas. The crystallization of sol IV, producing cristobalite despite the same fumed silica having been used, may be a consequence of the poor chemical homogeneity of the starting sol, which was prepared using three fumed powders. This is in contrast to sols I and II which were prepared using two nanosized powders and one colloidal solution. Poor mixing of sol IV has probably resulted in the formation of more AA and BB type clusters than the desired AB cluster. As a consequence the silica phase has been able to transform partially to cristobalite prior to mullitization. The same degree of non-mixing to form AB type clusters probably occurred in sol III. This sol was stable at a pH about 9, at which both the silica and alumina particles are negatively charged, thus resulting in reduced heterocoagulation and hence number of AB type clusters.

The best results in terms of final sintered density for the conditions investigated here were achieved for sols I and II. The lower densification achieved with sols III and IV may be attributed to their different crystallization behaviour, as discussed above, which showed the presence of cristobalite prior to mullite formation, thus hindering the viscous flow sintering mechanism of the amorphous silica, as frequently found in the literature.[18–20] The presence of very fine silica particles ($d_{av} \approx 12$ nm) with a very narrow particle size distribution (i.e. Aerosil 200) in sol II did not affect the densification behaviour significantly in comparison with sol I, in which larger silica particles ($d_{av} \approx 40$ nm) with a broader particle size distribution were used (i.e. Aerosil OX 50). At 1200°C, according to Table 2, the material is XRD amorphous (sol I) or only weakly crystalline due to the presence of δ-$Al_2O_3$ (sol II), and so densification can take place via viscous flow. This indicates that the preparation of 'composite' particles by coating alumina particles with a layer of silica particles is not strictly necessary for achieving near-full densification by transient viscous sintering of the pre-mullite powder compacts prepared from the commercial precursors used in the present work. At 1300°C, the samples achieved a density of 2·84 g cm$^{-3}$ (i.e. ≈90% of theoretical taking the theoretical density of mullite as 3·16 g cm$^{-3}$).[5] These densities can be improved, however, if hot-pressing is employed. It is envisaged, moreover, that when using hot-pressing for manufacturing composites, the mullite matrices derived from sols I and II may be densified fully at even lower temperatures. However, the effect of pressure on the densification and mullitization kinetics and their interaction, needs to be addressed and is the focus of current studies.

The study of the pressureless densification of compacts made from sol I powders has shown that an almost fully dense, monolithic mullite material can be obtained by sintering the green compacts at 1200°C for 2 h, followed by 5 h at 1450°C. This result is relevant for the preparation of monolithic mullite ceramics via conventional uniaxial pressing and pressureless sintering. Other authors have used much higher temperatures (up to 1700°C) to obtain dense mullite.[21,33–36] The possibility of densification by viscous flow may also be of importance for the development of dispersion-reinforced mullite ceramic composites, since an amorphous matrix sinters more easily around a dispersed reinforcement phase compared with a polycrystalline matrix.[37] In addition, the specimens sintered at 1450°C have a very fine equiaxed grain morphology, with a mean grain size of 0·8 μm. Since no elongated grains were formed, it can be concluded that there was no liquid phase formation during sintering after the viscous flow densification occurred.[38] Both the high degree of microstructural homogeneity and the fine grain size achieved suggest that the material may have interesting properties for load-bearing applications or for applications where infra-red transparency is required.[35]

## 5 Conclusions

Suitable commercially available alumina and silica precursors have been identified for the preparation of mullite ceramics via colloidal processing and

viscous transient sintering. These precursor materials also fulfil the requirements specified for the sol-based mullite matrix material to be used for infiltrating SiC woven fibre preforms using electrophoretic deposition. Owing to the lack of high-temperature thermal stability of the SiC fibres under investigation,[12,13] the processing temperature for manufacturing these composites is limited to ≈1300°C. At this temperature, the sintered density of the mullite matrices investigated in the present work is only ≈90% of theoretical. However, upon exploiting a viscous flow densification mechanism, it is envisaged that hot-pressing will produce fully dense mullite matrix composites at these relatively low temperatures. This is the subject of on-going studies. The simple pressureless sintering route developed using pre-mullite powders derived from sol I has demonstrated the production of dense (≈ 98% of theoretical density) monolithic mullite samples with a very fine, homogeneous microstructure at a sintering temperature of ≈1450°C.

## Acknowledgements

Professors J. F. Knott and M. H. Loretto are acknowledged gratefully for the provision of laboratory facilities in the School of Metallurgy and Materials and the IRC in Materials for High Performance Applications, respectively, at The University of Birmingham. Helpful discussions with Dr E. G. Butler are also appreciated. We also thank Degussa Ltd, UK for the Aerosil material. A.R.B. acknowledges the financial support of the European Commission via contract BRE2.CT94. 3064.

## References

1. *Mullite and Mullite Matrix Composites*, Ceramic Transactions. Vol. 6, eds S. Somiya, R. F. Davis & J. A. Pask. The American Ceramic Society. Inc., Westerville, OH, 1990.
2. Sacks, M. D. & Lee, H.-W., A review of powder preparation methods and densification procedures for fabricating high density mullite. *Ceram. Trans.*, **6** (1990) 167–207.
3. Aksay, I. A., Dabbs, D. M. & Sarikaya, M., Mullite for structural, electronic and optical applications. *J. Am. Ceram. Soc.*, **74** (1991) 2343–58.
4. Schneider, H., Merwin, L. & Sebald, A., Mullite formation from non-crystalline precursors. *J. Mater. Sci.*, **27** (1992) 805–12.
5. Jeng, D. & Rahaman, M. N., Effect of rigid inclusions on the sintering of mullite synthesized by sol–gel processing. *J. Mater. Sci.*, **28** (1993) 4421–6.
6. Zhou, Y., Vleugels, J., Laoui, T. & Van der Biest, O., Toughening of sol–gel derived mullite matrix by $Al_2O_3$ platelets. *J. Mater. Sci. Lett.*, **13** (1994) 1089–91.
7. Wu, M. & Messing, G. L., Fabrication of oriented SiC-whisker-reinforced mullite matrix composites by tape casting. *J. Am. Ceram. Soc.*, **77** (1994) 2586–692.
8. Wei, G. C. & Becher, P. F., Development of SiC-whisker-reinforced ceramic. *Am. Ceram. Soc. Bull.*, **64** (1985) 298–304.
9. Ho, C. T., In situ reacted $TiB_2$ reinforced mullite. *J. Mater. Sci.*, **30** (1995) 1338–42.
10. Mouchon, E. & Colomban, Ph., Oxide ceramic matrix/oxide fibre woven fabric composites exhibiting dissipative fracture behaviour. *Composites*, **26** (1995) 175–82.
11. Singh, R. N. & Gaddipati, A. R., Mechanical properties of a uniaxially reinforced mullite-silicon carbide composite. *J. Am. Ceram. Soc.*, **71** (1988) C-100–03.
12. Wu, J., Chen, M., Jones, F. R. & James, P. F., Mullite and alumina–silica matrices for composites by modified sol–gel processing. *J. Non-Cryst. Solids*, **162** (1993) 197–200.
13. Ha, J.-S. & Chawla, K. K. Mechanical behaviour of mullite composite reinforced with mullite fibres. *Mater. Sci. Eng.*, **A203** (1995) 171–6.
14. Boccaccini, A. R., Taplin, D. M. R., Butler, E. G., Marquis, P. M. & Ponton, C. B., Manufacturing of ceramic matrix composites via electrophoretic deposition. In *Proc. 4th EUROMAT Conference*, Venice/Padua, Italy, 25–28 September 1995, pp. 325–30.
15. Boccaccini, A. R. & Ponton, C. B., Processing ceramic-matrix composite using electrophoretic deposition. *J. Met.*, **47**[10] (1995) 34–7.
16. Illston, T. J., *et al.*, UK Patent 9124822.9, 1991.
17. Sacks, M. D., Bozurt, N. & Scheiffele, G. W., Fabrication of mullite and mullite-matrix composites by transient viscous sintering of composite powders. *J. Am. Ceram. Soc.*, **74** (1991) 2428–37.
18. Shyu, J.-J. & Chen, Y.-C., Zirconia–mullite ceramics made from composite particles coated with amorphous phase: I Effect of zirconia addition. *J. Mater. Res.*, **10** (1995) 63–70.
19. Wang, J., Piramoon, M. R., Ponton. C. B. & Marquis, P. M., Sol–gel processing of monolithic and composite mullite ceramics. In *Nanoceramics*, ed. R. Freer. Br. Ceram. Proc. No. 51, 117–33.
20. Wang, J., Piramoon, M. R., Ponton, C. B. & Marquis, P. M., Fabrication and microstructure–property relationships in the transiently/reaction sintered mullite composites. *Proc. Euromat 91*, eds T. W. Clyne & P. J. Withers. The Institute of Materials, Vol. 2, (1991), pp. 287–99.
21. Miao, X., Ponton, C. B. & Marquis, P. M., Production of mullite nanoceramics through controlled heterocoagulation of sols. In *Nanoceramics*, ed. R. Freer. Br. Ceram. Proc. No. 51, 1993, pp. 157–64.
22. Wang, J. G., Ponton, C. B. & Marquis, P. M., Effects of green density on crystallization and mullitization in the transiently sintered mullite. *J. Am. Ceram. Soc.*, **75** (1992) 3457–61.
23. Huling, J. C. & Messing, G. L., Surface chemistry effects on homogeneity and crystallisation of colloidal mullite sol–gels. *Ceram. Trans.*, **6** (1990) 220–8.
24. Komarneni, S. & Roy, R., Mullite derived from diphasic nanocomposite gels. *Ceram. Trans.*, **6** (1990) 209–19.
25. Huling, J. C. & Messing, G. L., Hybrid gels for homoepitactic nucleation of mullite. *J. Am. Ceram. Soc.*, **72** (1989) 1725–9.
26. Trusty, P. A., Boccaccini, A. R., Butler, E. G. & Ponton, C. B., Novel techniques for manufacturing woven fibre reinforced ceramic matrix composites. *Mater. Manuf. Processes*, **6** (1995) 1215–26.
27. Boccaccini, A. R., Engineered fibre strengthened ceramic composites: structural integrity and performance in energy conversion and processing systems. Quarterly Report), submitted to DG XII-Brussels, April 1995.
28. Clasen, R., Electrophoretic deposition of compacts of nano-sized particles. In *Science, Technology and Applications of Colloidal Suspensions, Ceram. Trans.* Vol. **54**. The American Ceramic Society, Westerville, OH, 1995, pp. 169–84.
29. Hsi, C.-S., Lu, H.-Y. & Yen, F.-S., Thermal behaviour of alumina–silica xerogels during calcination. *J. Am. Ceram. Soc.*, **72** (1989) 2208–10.

30. Okada, K. & Otsuka, N., Characterisation of the spinel phase from $SiO_2$–$Al_2O_3$ xerogels and the formation process of mullite. *J. Am. Ceram. Soc.*, **69** (1986) 652–6.
31. Okada, K. & Otsuka, N., Formation process of mullite. *Ceram. Trans.*, **6** (1990) 375–387.
32. Lee, J. S. & Yu, S. C., Mullite formation kinetics of coprecipitated $Al_2O_3$–$SiO_2$ gels. *Mater. Res. Bull.*, **27** (1992) 405–16.
33. Kanka, B. & Schneider, H., Sintering mechanisms and microstructural development of coprecipitated mullite. *J. Mater. Sci.*, **29** (1994) 1239–49.
34. Ismail, M. G., Nakai, Z. & Somiya, S., Microstructure and mechanical properties of mullite prepared by the sol–gel method. *J. Am. Ceram. Soc.*, **70** (1987) C-7–C-8.
35. Mroz, T. & Laughner, J. W., Microstructures of mullite sintered from seeded sol–gels. *J. Am. Ceram. Soc.*, **72** (1989) 508–9.
36. Hilz, G. & Ziegler, G., Reaction-sintered and reaction-hot-pressed mullite prepared from mixtures of commercial $Al_2O_3$- and $SiO_2$-powders. In *Fourth Euro Ceramics*, Vol. 4. ed. A. Bellosi. 1995, pp. 479–86.
37. Bordia, R. K. & Raj R., Analysis of sintering of a composite with a glass or ceramic matrix. *J. Am. Ceram. Soc.*, **69** (1986) C55–C57.
38. Kara, F. & Little, J. A., Sintering of pre-mullite powder obtained by chemical processing. *J. Mater. Sci.*, **28** (1993) 1323–6.